Ecological Engineering & Environmental Technology, 2025, 26(12), 302–320 https://doi.org/10.12912/27197050/214189 ISSN 2719–7050, License CC-BY 4.0

Sustainable conversion of agricultural waste to activated biochar: Optimization and modelling of methylene blue adsorption

Soukaina Nehhal¹, Majda Ben Ali¹, Younes Abrouki¹, Khalid Ofqir¹, Yassine Elkahoui¹, Souad El Hajjaji^{1*}

- ¹ Laboratory of Spectroscopy, Molecular Modeling, Materials, Nanomaterials, Water and Environment (LS3MN2E), Department of Chemistry, Faculty of Sciences, Mohammed V University in Rabat, Morocco
- * Corresponding author's e-mail: souad.elhajjaji@fsr.um5.ac.ma

ABSTRACT

This research investigated the transformation of agricultural waste into useful materials employed for wastewater adsorption treatment containing textile dyes. The synthesized materials underwent various analysis to investigate their physicochemical characteristics. It was shown in Fourier-transform infrared spectroscopy that Surfaceactive functional moieties have changed, while X-ray diffraction demonstrated changes to the mineral structure. The hydroxyde de potassium activated sample showed highly developed porous microstructure, and scanning electron microscopy morphology was corresponding to a high Brunauer-Emmett-Teller, Surface development of $108,022 \, \mathrm{m^2/g}$. The optimization of operational parameters was executed by a statistical approach based on a central composite design. A significant association between the measured data and the pseudo-first-order model was observed was a good descriptor and supported the hypothesis that the adsorption occurred via a physisorption mechanism. Moreover, the Sips isotherm model reflected an excellent fit to the equilibrium data. These findings demonstrate the strong potential of the developed materials for methylene blue adsorption and support their application in water treatment processes.

Keywords: agricultural waste, surface area, activated carbon, adsorption, thermochemical treatment, activated carbon with potassium hydroxide.

INTRODUCTION

Agricultural waste management is becoming an ever-increasing environmental challenge, especially because the volumes of residues resulting from agricultural intensification are on the rise (Riseh et al., 2024; Wang and Cui, 2024). These waste products are often left to rot in the field, or, even worse, open burning which contributes to air pollution with CO₂, CH₄, and particulates, as well as reducing soils viability and polluting groundwater (Cao et al., 2023; Escudero-Curiel et al., 2023). The uncontrolled build-up of organic residues and wastes increases the burden of pathogens, pests, and diseases including those relevant to public health (Van Den Broek et al., 2024). With this background, sustainable valorization of agricultural biomass (and in particular, agricultural waste biomass, or a more restricted definition of residues, such as artichoke and cardoon residues will represent a sustainable short-solution, or rotational solution, as there are abundant supplies of heavy lignocellulosic plant residues (Cao et al., 2023; Escudero-Curiel et al., 2023). These include cellulose, hemicellulose, lignin, and bioactive compounds – flavonoids and phenolic acids, and represent a superior feedstock for this production. Thermochemical conversion processes are differentiated from other valorization processes by its ability to convert organic waste into energy, or useful materials (Unyay et al., 2025; Mujtaba et al., 2023; Castagna et al., 2025). Thermochemical conversion processes include gasification (Seo et al., 2022; Maitlo et al., 2022), combustion (Liu et al., 2025), hydrothermal carbonization (Czerwińska et al., 2022),

Received: 2025.10.19 Accepted: 2025.11.15

Published: 2025.12.01

and pyrolysis (Giertl et al., 2024), which at this time appears to be the most practical option for materials recovery. In pyrolysis, organic matter is affected by high temperatures under oxygen-free conditions, causing its decomposition, usually between 300-700 °C (Al-Rumaihi et al., 2022; Ippolito et al., 2020; Kuryntseva et al., 2023). Thermally decomposed biomass residue has gained intensifying interest as a consequence of to unique characteristics (Yaashikaa et al., 2020; Dong et al., 2024; Ben Ali et al., 2025). A number of activation processes could be applied to optimize the biochar product. Physical activation involves high temperature using steam or CO, that can increase porosity and specific surface area, but chemical activation can enhance or enable targeted functional properties beyond what would be achievable for physical activation using some activating agents (Sun et al., 2024; Fakhar et al., 2025a). For alkaline activating agents like KOH and NaOH, surface area can greatly increase which in the case of KOH can generate a microporosity that is well above 1000 m²/g, form internal channels because of layer spacing and etching of carbonaceous matrix, and create basic surface sites for the adsorption of acidic compounds (Fakhar et al., 2025b; Ben Ali et al., 2025). Likewise, the mineral acids H₂PO₄, H₂SO₄, and HCl work by hydrolyzing the lignocellulosic matrix, stabilizing the aromatic structures, and removing the remaining ash in the biomass (Ben Ali et al., 2025). Consequently, the thermochemical transformation by pyrolysis of the waste from artichokes and cardoons combined with physical or chemical activation provides a novel sustainable option for multimodal materials (Amer et al., 2021). The method completely promotes Leveraging circular economy strategies to lessen the ecological burden of agricultural waste while generating beneficial strategies for resource reclamation and remediation of contaminated environments (Perdana et al., 2023; Islam et al., 2024). Biochar that have been activated, have demonstrated themselves to be very effective adsorbents for dye removal from industrial effluents, given their well developed porosity, significant High surface area and rich surface-active sites functional moieties to interact with colored organic molecules (Trivedi et al., 2025; Wu et al., 2020; Srivatsav et al., 2020). Amongst these dyes methylene blue is often utilized as a model compound in adsorption experimentation due to its chemical stability (Al-Asadi et al., 2025;

Eyupoglu et al., 2025). Regardless of the significance of methylene blue in industry it is not without risk to the environment, as an environmentally hazardous pollutant due to biota toxicity representing a risk Influencing aquatic biota and human health (Oladoye et al., 2022). Adverse exposure to methylene blue can include effects on the respiratory, nervous, and digestive systems, in addition to irritating mucous membranes (Khan et al., 2022). Methylene blue is particularly abundant in wastewater and its structural composition makes it resistant to biodegradation, and difficult to remove with traditional wastewater treatment methodologies (Li et al., 2025).

In this case, activated biochar provide an economical, appealing, and environmentally friendly sound approach for efficient adsorption methylene blue removal from water-based solutions. The presence of well-developed micropores along with a base-modified surface (using NaOH or KOH), thus providing rapid and effective adsorption (Mu et al., 2022). The methodology enables wastewater purification while also providing a solution to orgainc waste valorization by thus contributing to the sustainable management of a resource within the environment, while effectively curbing pollution load on the environment (Wang and Shafieezadeh, 2025). The use of activated biochar can be a beneficial and low-cost option for efficiently taking up methylene blue in water at practical doses. Activated biochar, which refers to a material derived from activated carbon, and is defined as being derived from micropores, creating a basic surface as a result of alkaline activation in NaOH or KOH that encourages a mixed charge. The synergistic interactions led to rapid and efficient uptake of methylene blue to not only assist in purifying contaminated water, but also to contribute to the valorization of large quantities of organic waste, helping to promote sustainable resource management while also decreasing the total environmental pollutant load (Genuino et al., 2018; Dang et al., 2023).

This study is framed in relation to an innovative dimension of using agricultural waste as a form of valorization as we transition to a circular and sustainable economy and focusing specifically on artichoke and cardoon agricultural waste. But the vast majority of agricultural residues, like many others, are often seen as an undervalued biodegradable resource and in this study, we attempt to convert this waste into more highly esteemed functional materials as a result of a thermochemical transformation

process. The study uses a thermochemical path that rigorously optimizes and characterizes both the pyrolysis and any possible post pyrolization processes. This novel approach of harvesting value from waste materials differs from the existing thermal treatments of biomass using pyrolysis in that it comprises of both the thermal conversion of the feedstock into biochar via a pyrolysis stream and a post-pyrolysis sequence that comprises washing the biochar with hydrochloric acid (HCl) and subsequently activated through a potassium hydroxide treatment. The HCl washing step allows for selective demineralization of the raw biochar through the extraction of residual ash and mineral fractions that would block pore structure and impede the adsorptivity of the material thus facilitating the construction of the pore network in the activation step. Chemical activation using KOH improves specific surface area, and enlarges both micro and mesoporosity, and creates active chemical sites by adding new Oxygenated functional moieties present at the surface of the biochar. This study also considered a key consequence of chemical activation that has been underappreciated in previous studies: the crystallization of mineral compounds, such as K₂CO₃, Ca (OH), and MgO in our study, which occurred during thermochemical treatment in presence of KOH. The newly formed crystalline phases may act synergistically to improve the surface reactivity of the total material.

While many studies incorporate only chemical activation, we present a combined procedure of acid demineralization and alkaline activation that address and improves the textural and chemical properties of biochar more effectively. Additionally, our combined approach minimizes the excessive use of corrosive reagents and boosts the material's overall effectiveness. Modern statistical modeling methods, specifically Response Surface Methodology, has served to improve process variables for optimizing the adsorption behavior of the material. Ultimately, an extensive range of physicochemical tests (FTIR, XRD, SEM, BET surface area) were performed to characterize structural and chemical changes occurring within the biochar throughout the entire process. This investigation thus offered a sustainable, cost-effective, and relevant scientific strategy for the smart conversion of agricultural wastes into high-performance adsorbents, while also contributing towards the amelioration and reduction of the environmental cost of managing our organic waste disconnect.

MATERIALS AND EXPERIMENTAL APPROACH

Valorization of agricultural residues into activated carbon

Activated biochar was obtained from agricultural residues through a staged procedure, described in Figure 1. First, the agricultural waste is ground the sample was dried (105 °C) for one night. The waste is then subjected to pyrolysis in a programmable thermal treatment was carried out at 700 °C for 60 minutes, with a controlled ramp

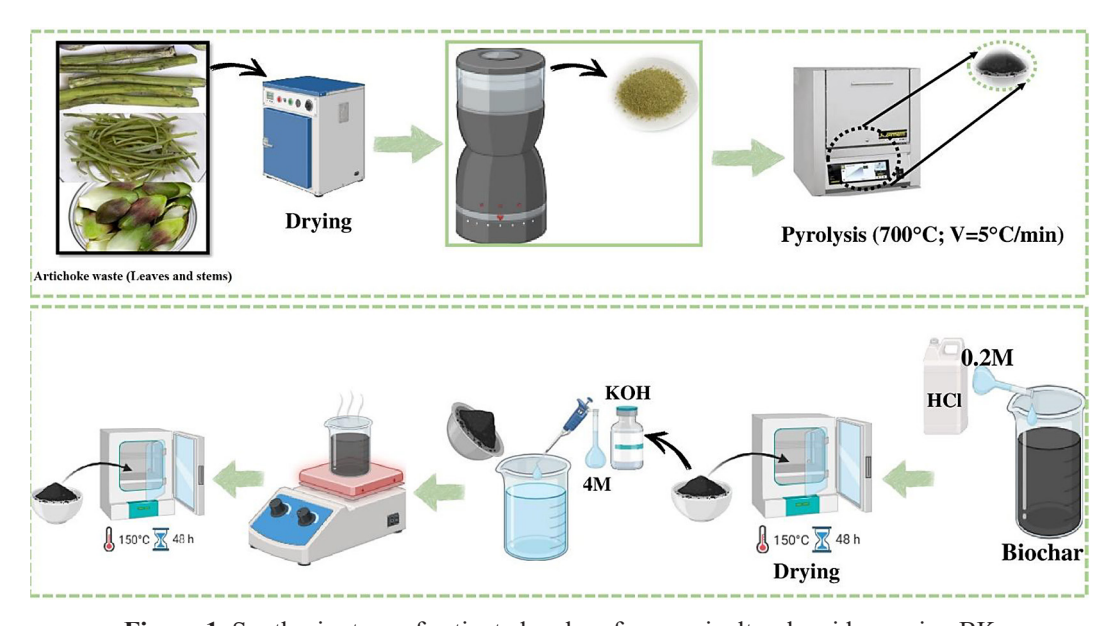


Figure 1. Synthesis steps of activated carbon from agricultural residues using BK

of 5 °C per minute. The resulting raw biochar is washed four times with hydrochloric acid (HCl) solution (0.2 M), neutralized, and then dried.

Subsequently, 10 grams of this biochar are chemically activated using a 4 M KOH solution under sonication at 70 °C for two hours, then neutralized and dried to obtain the activated biochar.

Characterizations

Surface area measurement (BET Method)

To measure the surface area, the samples were preheated at 350 °C under vacuum to remove any moisture or gases trapped in the pores. Then, they were placed in a sealed tube and cooled with liquid nitrogen at 77 K. Nitrogen gas was passed over the sample at different pressures, and the amount of gas that stuck to the surface was measured using a NOVA 2200 analyser. The results were calculated automatically using the BET method, which gives information about.

Identification of functional groups (FTIR)

A Nicolet iS50 spectrometer was used for FTIR analysis to characterize the surface chemical functionalities of the activated carbon. The data were recorded from 400–4000 cm⁻¹, with a scanning resolution of 4 cm⁻¹.

Surface morphology and composition

SEM analysis was conducted to characterize the microstructure of the sample, and conducted elemental composition analysis using the elemental composition was analyzed by energy-dispersive X-ray spectroscopy (EDX) on a QUATTRO S-FEG system (Thermo Fisher)

Crystalline structure

The crystalline structure was analyzed by XRD using a Shimadzu 6100 diffractometer with a scanning speed of 2° /min over the $10-70^{\circ}$ (2θ) range.

Determination of the surface charge neutrality point

Surface charge evaluation is an important step in material characterization, as this helps to find each material's point of pH_{pzc}. In this study, several solutions of sodium chloride were made at 50 mL, prepared as a 0.01 M solution with pH

values spanning 2–12. To the sodium chloride solutions, we added 0.15 g of each the materials in question. The various mixtures were agitated for 48 h to reach equilibrium. The pH of the filtrate from each mixture was then taken to understand the zeta potential of the surface behaviour of the materials (Rivera-Utrilla et al., 2001). The pHpzc was determined using the Equation 1.

$$\Delta pH = pH_{f} - pH_{i} \tag{1}$$

where: pH_f representing the final pH and pH_i denoting the pH value at the start of the experiment.

ADSORPTION EXPERIMENTS

Chemically activated biochar using KOH was investigated for its adsorption efficiency. A With a loading of 0.6 g/L was applied to 50 mL of the methylene blue solution Prepared at 60 mg/L. For three hours, the mixture was continuously shaken at room temperature. To allow adsorption equilibrium, followed by filtering the solutions and then added to a UV–visible spectrophotometer for the remaining dye content at a wavelength of 664 nm.

Utilization of experimental design

The experimental framework, the study used a central composite design (CCD), which is a common experimental design that can be appropriately used to study adsorption processes. We used CCD to simulate the adsorption behavior of MB as the adsorbates for the synthesized adsorbents. The complete set of experiments (N) for the study was calculated as follows (Asfaram et al., 2015):

$$N = 2k + 2 \times k + N0 \tag{2}$$

In this experimental framework, k indicates the number of variables and N₀ represents the center point replicates performed in triplicate, to provide an indication of the accuracy and consistency of the measured results. Experimental design and analysis was performed in Design Expert to analyse the experimental data. The ranges and levels for each variable are listed in Table 1.

Adsorption equilibrium modelling

An effective Designing an adsorption system requires upon knowledge garnered from adsorption isotherms that evaluate the equilibrium

Variables	Predictor variables					
	Lineard and visit in land (V.)	Unit	Coded settings of factor X			
	Uncoded variables (X _i)	Offic	Lower level	Center	High level	
Input	X ₁ = treatment time	min	80	115	150	
variables	X ₂ = mass of adsorbent	g/L	0.2	0.6	0.9	
	X ₃ = solution pH		6	7	8	
	X ₄ = concentration of the dye in solution	ppm	40	60	80	
Output variable	Responses					
	Y = adsorption performance (mg/g)					

Table 1. Parameters influencing and derived from the adsorption process

interactions between adsorbate molecules in solution and solids surfaces. The isotherm illustrates the relationship between the adsorbate amount on the adsorbent (q_e) and the equilibrium concentration of the adsorbate in solution. (C_e) in some mathematical fashion. The equilibrium data obtained experimentally were fit to several common isotherm models including Langmuir, Freundlich, and Sips.

Adsorption is considered to occur according to the Langmuir isotherm model uniformly on a homogenous surface upon which a monolayer of adsorbate is formed. The model is commonly represented with the following expression (Morosanu et al., 2020):

$$q = \frac{q_m K_L C_e}{1 + C_e K_L} \tag{3}$$

where: q_m (mg.g⁻¹) indicates the calculated adsorption capacity at saturation, and K_L (L.mg⁻¹) denotes the Langmuir constant. The Freundlich isotherm considers adsorption as a reversible, multilayer process occurring on heterogeneous surfaces and ignores interactions between the adsorbed species, (Morosanu et al., 2020).

The following mathematical equation represents the Freundlich isotherm:

$$q = K_F C_e^{\frac{1}{n}} \tag{4}$$

In the Freundlich isotherm, K_F ((mg/g) (mg/L)-1/n) indicates the capability for adsorption constant, and 1/n is an empirical parameter of the adsorption performance or the surface diversity. The Sips isotherm, more commonly referred to as the Langmuir–Freundlich model, incorporates elements of adsorption on heterogeneous surfaces

can be well represented by both the Langmuir and Freundlich isotherms. surfaces with adsorbed molecules capable of binding to multiple sites. This isotherm does not account for interplay between adsorbed molecules (Shikuku and Jemutai-Kimosop, 2020a). The Sips isotherm, represented mathematically in the following way:

$$q = \frac{q_m K_S C_e^{n_S}}{1 + K_S C_e^{n_S}} \tag{5}$$

where: K_s (L/g) is used to denote the binding affinity constant while n_s represents the heterogeneity factor of the system.

In general, larger ns values indicate increased surface heterogeneity and ns values approaching one suggest a more homogeneous adsorbent surface which agrees with the theoretical basis of the Langmuir model (Shikuku and Jemutai-Kimosop, 2020a).

Study of adsorption kinetics

The comprehension of the adsorption mechanism relies mainly on kinetic studies in which the both pseudo-first-order and pseudo-second-order models are applied to often utilized (Tangarfa et al., 2019). Adsorption kinetics are represented by the pseudo-first-order model and demonstrates the sorption kinetics designed under a first-order reaction, and it can be expressed mathematically by the equation as follows (Tekin et al., 2010):

$$q = q_e \left(1 - e^{-k_1 t} \right) \tag{6}$$

where: qe and q (mg.g⁻¹) stand for the amounts of adsorbate adsorbed at equilibrium and at some selected time, t (minutes), respectively; K_1 (min⁻¹) is the rate constant of first-order adsorption kinetics.

The pseudo-second-order kinetic model posits that the adsorption process is dependent on both chemical and physical interaction between the adsorbate and adsorbent. This is represented as follows:

$$q = \frac{k_2 q_e^2 t}{1 + k_2 q_e t} \tag{7}$$

The corresponding parameter k_2 (min⁻¹) indicates the rate constant for adsorption based on second-order kinetics. The intraparticle diffusion stage can be expressed mathematically using Equation 8 (Campos et al., 2018):

$$Q_{t} = K_{p} + t^{1/2} + C \tag{8}$$

where: Q_t denotes the adsorption capacity at time t (mg. g⁻¹), K_p is the intraparticle diffusion rate constant (mg. g⁻¹.min^{-1/2}), and C accounts for the boundary layer thickness.

RESULTS

Evaluation of activated carbon characteristics

FTIR-based structural analysis

Figure 2 displays the FTIR spectra of agricultural waste, biochar, and KOH-activated carbon (BK). For the raw biomass, a band at 3066.08 cm⁻¹

is characteristic of –OH groups involved in hydrogen bonding. Absorption occurs at 2722.62 cm⁻¹ and 2430 cm⁻¹ correspond to the stretching vibrations of aliphatic hydrogen–carbon groups.

The peak identified at 1701.24 cm⁻¹ is a distinctive feature linked to carbonyl (C=O) moieties, with the peak at 1417.42 cm⁻¹ being related to the stretching of carbon-carbon double bonds in aromatic rings. The band at 1222 cm⁻¹ is probably from C-O stretching vibrations typically exhibited by carboxylic acids, and the peak at 1011.1 cm⁻¹ could also be related to similar vibrational stretching of the carbonyl group. The peak around 882.21 cm⁻¹ shows elongation vibrations of silicon-oxygen bonds, evidencing the presence of silaceous compounds (Bencheikh et al., 2020; Hajji Nabih et al., 2021; Alghuthaymi, 2025). Following pyrolysis, a significant drop or disappearance of many of the characteristic bands is observed, which indicates the degradation under heat of labile organic functional groups and the gradual aromatization of the carbon structure. Upon chemical activation with KOH, the FTIR spectrum of BK reveals the reappearance of bands associated with hydroxyl groups, confirming the successful incorporation of oxygenated surface functionalities (ElShafei et al., 2017; Ma et al., 2018).

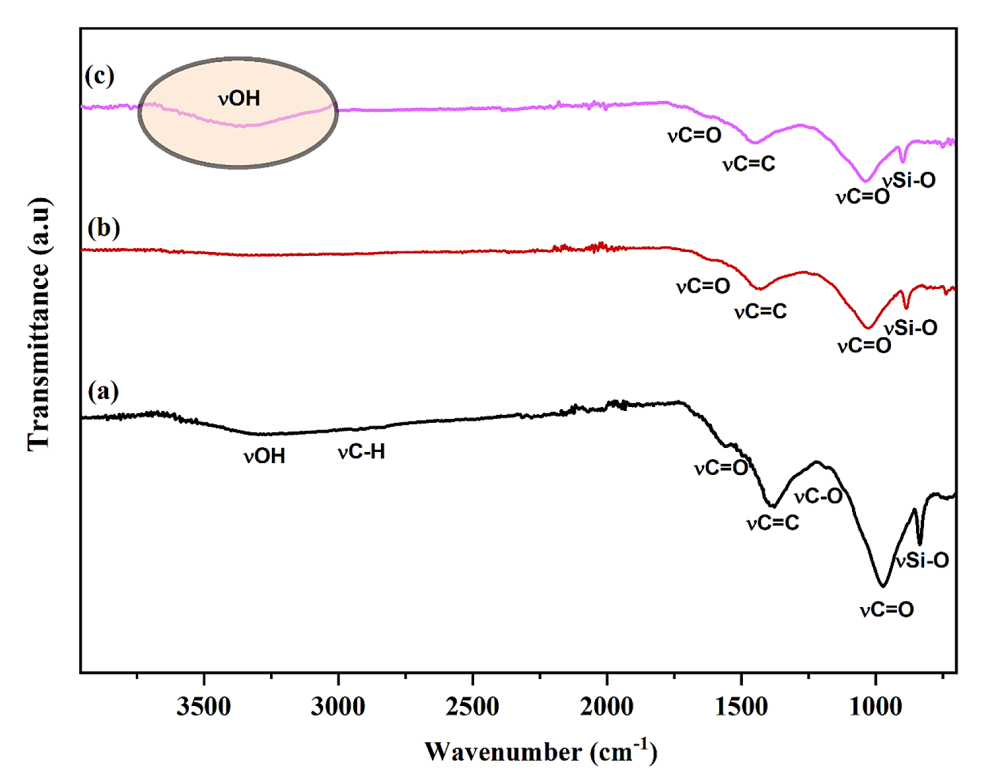


Figure 2. FTIR spectra of untreated agricultural by-products (a), biochar (b), and BK (c)

pH of zero-point charge

Figure 3 presents the experimental determination of the point of pH_{pzc} for the different adsorbent materials, including raw agricultural waste, biochar, and KOH-activated biochar (BK). The raw precursor had a pH_{pzc} of 7.79, which marginally increased to 8.04 after pyrolysis. This can be Due to heat-induced breakdown of organic material and loss of acidic surface groups, including hydroxyl and carboxyl functionalities. Following chemical activation with KOH, the pH_{pre} slightly decreased to 7.90, likely due to modifications in surface chemistry induced by the activating agent. From a mechanistic perspective, A solution pH above the pH_{pzc} results in a negatively charged adsorbent surface, promoting electrostatic attraction toward cationic species (Bencheikh et al., 2021).

Morphological investigation by SEM

The surface morphology of untreated agricultural waste and its changes from pyrolysis and KOH activation was characterized by SEM. The mineral and organic heterogeneity of the untreated biomass is exhibited in Figure 4a, which depicts micrometer-sized plates with irregular aggregates (this is typical of lignocellulosic biomass) (Guan et al., 2023). The changes in surface morphology after pyrolysis and KOH chemical activation are demonstrated in Figure 4b. The surface shows distinct porosity with interconnected pores and

cavities produced by gaseous and volatile species during thermal and chemical etching (Gómez et al., 2022; Kim et al., 2023). Ultimately, due to the pronounced porosity, the activated biochar shows an increased surface area and adsorption capacity to enhance its reactivity and catalytic or adsorptive efficacy.

Evaluation of specific surface area and porosity using BET

Figure 5 depicts the behavior of nitrogen adsorption and desorption of raw agricultural waste, pyrolyzed-biochar, and biochar treated with KOH (BK). The isotherm of the agricultural waste is consistent with a Type I isotherm based on IUPAC classification; meaning that the material is a micropore material with a low external surface area, which is shown by the small Adsorption-desorption loop. This type of isotherm type is commonly related to monolayer adsorption, and is consistent with the Langmuir adsorption model. Alternatively, the activated biochar (Figure 5c) displays a mixed isotherm with both Type I and Type IV characteristics. The data shows micropores and mesopores. The sharp increase in adsorbed gas at low relative pressures and the hysteresis loop shown by the capillary condensation indicates the presence of mesoporous structures. According to Boer's classification, the hysteresis loop is categorized as Type B since its adsorption branches

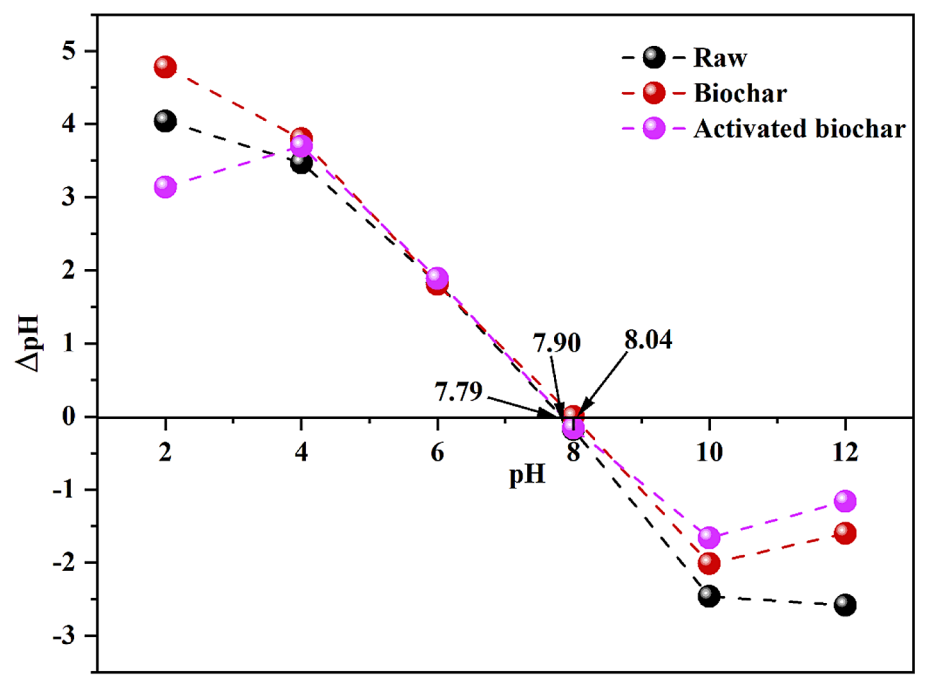


Figure 3. Influence of surface charge characteristics

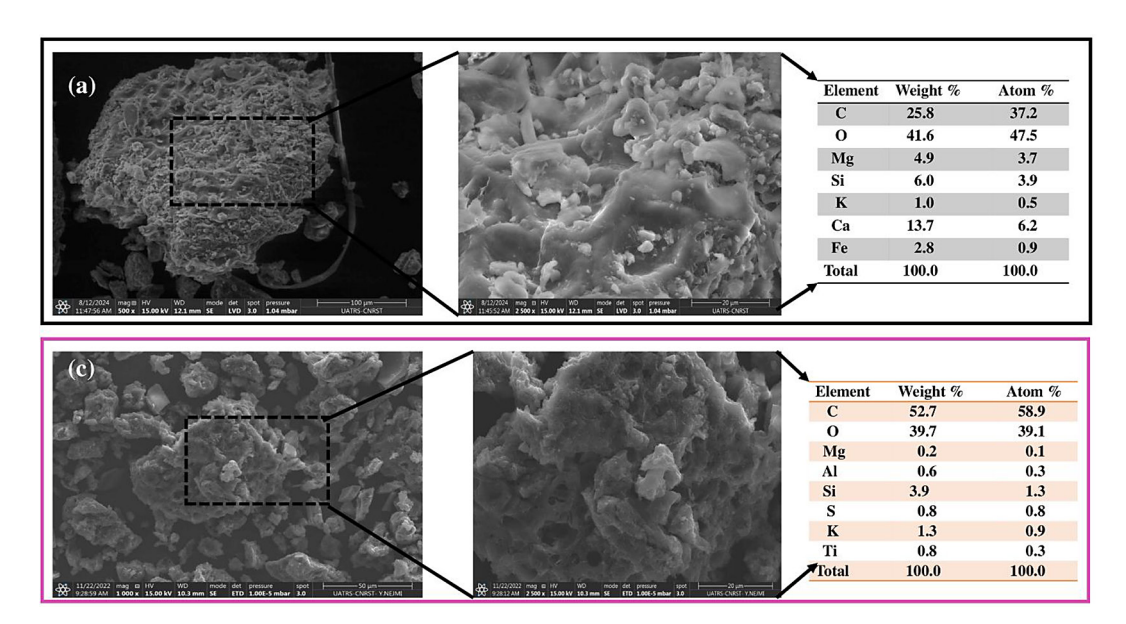


Figure 4. SEM/EDX characterization of (a) agricultural waste, and (c) BK

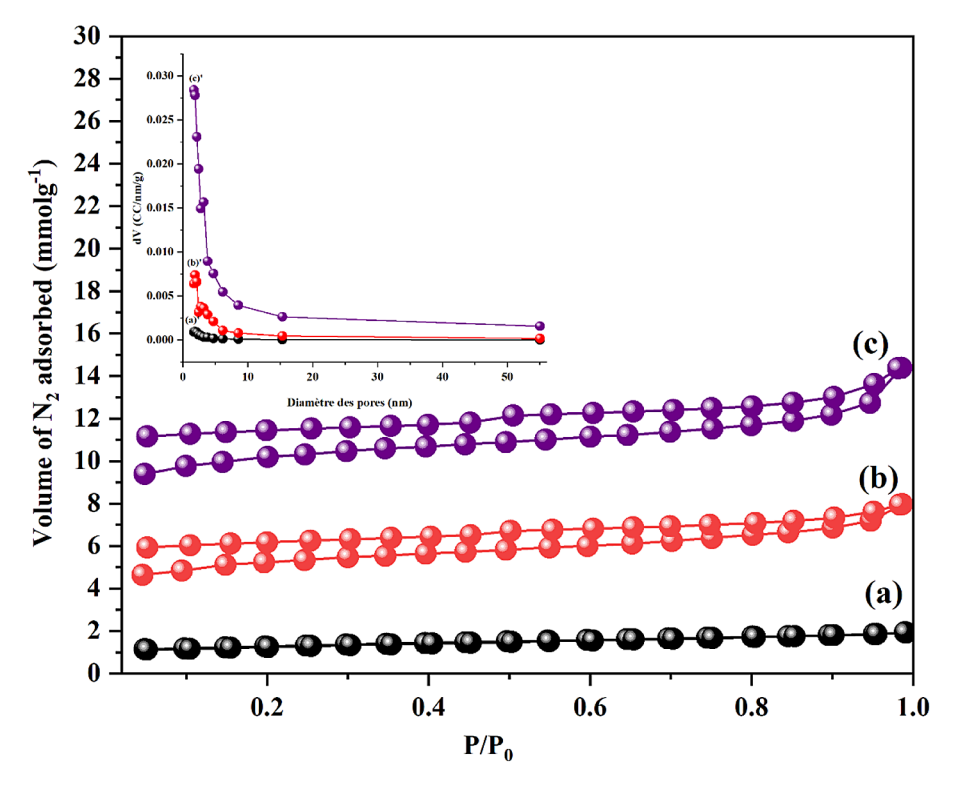


Figure 5. Nitrogen adsorption—desorption profiles depicting pore volume development in: (a) raw agricultural waste, (b) biochar, and (c) BK

around the saturation pressure are steep. The existence of hysteresis during desorption is indicative of a more complicated pore structure, including both micropores and mesopores. In contrast, the adsorption and desorption curves for the raw agricultural waste, overlap nearly entirely and exhibited relatively no hysteresis, which indicates that the specific surface area is minimal. The activation

of KOH greatly increased the micropore volume and total pore volume, summarized in Table 2. The pore size distribution presented in Figure 6, from the BJH method on the various materials, shows the raw sample (a), biochar (b), and KOH-activated biochar (c). We can see there is a significant increase in the pore volume between 1–2 nm after chemical activation, indicating enrichment

of micropores. Furthermore, the development of mesopores in the 2–10 nm range is much more pronounced during pyrolysis and KOH activation (Aguiar et al., 2014; ElShafei et al., 2017). Table 2 shows the distinct development of specific surface areas during the treatment process. The raw agricultural waste material demonstrates an extremely low surface area. However, the chemical activation with KOH substantially increases the total surface area to as high as 108.022 m²/g. In addition, the microporous surface area substantially expands from 4.022 m²/g to 80.041 m²/g after treatment.

X-ray diffraction-based structural characterization

As shown in Figure 6, a mineralogical analysis is presented for the raw agricultural waste, the biochar, and the KOH activated biochar (BK) (Figure 6c). The X-ray diffraction pattern of the raw agricultural waste (Figure 6(a)) identifies the signature mineral phases quartz and dolomite. The

broad hump between $15\text{--}35^\circ$ (2θ) suggests some presence of amorphous organic matter. It is likely that the presence of quartz originates from the clay and sand fractions. Calcium carbonate (CaCO₃) likely originates from the dolomitic fraction associated with the sandy materials (Bencheikh et al., 2020 ; Chen et al., 2023 ; Nematallah et al., 2024). Pyrolysis at 550 °C (Figure 6(b)) and a subsequent acid wash with hydrochloric acid show a significant reduction in mineral content. Following chemical activation with KOH (Figure 6(c)), we find several new crystalline phases such as K_2CO_3 , MgO, and $Ca(OH)_2$ (Barakat et al., 2024; Lendzion-Bieluń et al., 2018).

RESPONSE SURFACE METHODOLOGY

Table 3 displays the results from 26 experimental trials involving four independent parameters. The relationship between factors and responses

TO 1 1 A 3 4 1'C' 4'	C /1 / 1	. C. C	1
Table 2. Modification	of the material	s specific siirface and	nore space volume
Tuble M. Modification	or the material	specific surface and	pore space voranie

Parameter	BET surface area (m²/g)	Internal surface area of micropores (m²/g)	Pore volume (cm³/g)	Micropore volume (cm³/g)
Untreated	6.789	4.022	0.0077	0.0066
Biochar	50.0213	22.006	0.0761	0.0522
BK	108.022	80.041	0.2567	0.20165

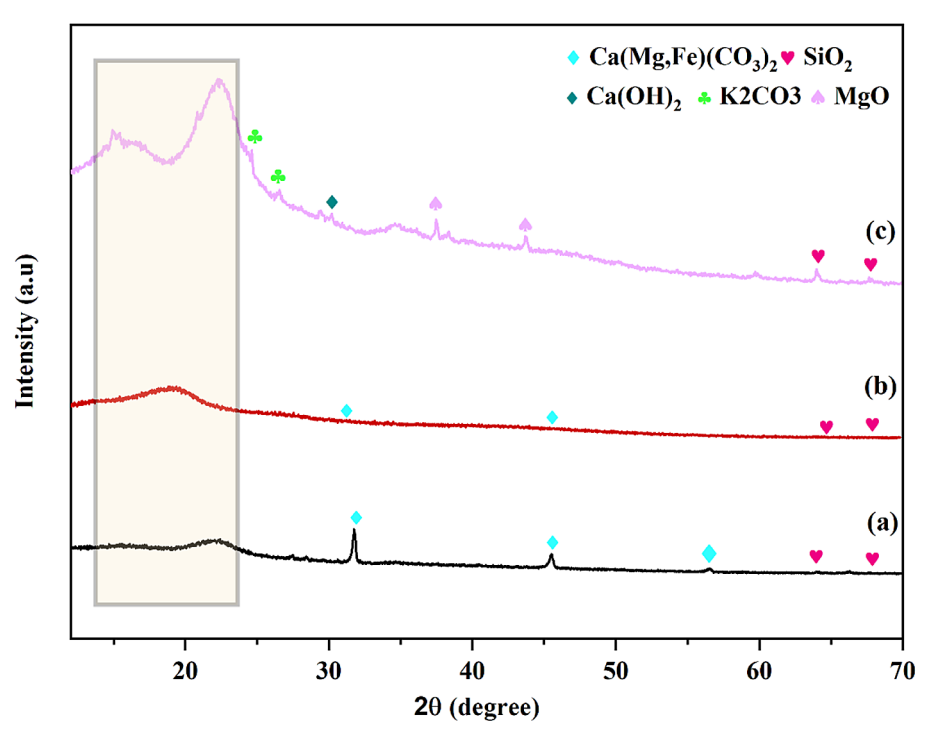


Figure 6. analysis results of (a) raw agricultural waste, (b) biochar, and (c) BK

No.	X ₁	X_2	X ₃	X ₄	Reponses
1	1	1	-1	-1	66.59
2	1	1	-1	1	55.1
3	1	1	1	-1	26.96
4	1	1	1	1	64.24
5	1	-1	-1	-1	53.46
6	1	-1	-1	1	74.41
7	1	-1	1	-1	155.4
8	1	-1	1	1	100.79
9	-1	1	-1	-1	78.59
10	-1	1	-1	1	93.64
11	-1	1	1	-1	13.99
12	-1	1	1	1	90.54
13	-1	-1	-1	-1	62.11
14	-1	-1	-1	1	199.79
15	-1	-1	1	-1	77.55
16	-1	-1	1	1	168.3
17	-2	0	0	0	79.04
18	2	0	0	0	91.47
19	0	-2	0	0	97.45
20	0	2	0	0	62.23
21	0	0	-2	0	55.41
22	0	0	2	0	182.84
23	0	0	0	-2	96.95
24	0	0	0	2	11.4
25	0	0	0	0	62.23
26	0	0	0	0	81.47

Table 3. Experimental design using coded levels and observed adsorption results

was characterized through a quadratic polynomial expression, presented in the following form:

$$\begin{array}{c} Q = 72.82 + 1.39 X_{1} - 31.99 X_{2} + 1.28 X_{3} + 1 \\ + 6.14 X_{4} + 1.99 X_{1} X_{2} + 9.62 X_{1} X_{3} - 14.61 X_{1} X_{4} - \\ - 8.81 X_{2} X_{3} - 17.10 X_{2} X_{4} + 12.80 X_{3} X_{4} + 2.4 \\ - 7 X_{12} + 14.46 X_{22} + 5.28 X_{32} - 9.34 X_{42} \end{array} \tag{9}$$

From this equation, it can be observed that the reaction time, the pH of MB, and the MB concentration positively influence the adsorption efficiency, whereas the adsorbent mass has a negative effect. Furthermore, the interactions between reaction time and adsorbent mass, reaction time and pH, as well as pH and methylene blue concentration also have a positive impact. Conversely, the interactions between reaction time and MB concentration, adsorbent mass and pH, and adsorbent mass and methylene blue concentration negatively affect the adsorption efficiency. Regarding the quadratic terms, those related to reaction time, adsorbent mass,

and methylene blue pH exhibit positive effects, while the quadratic term of methylene blue concentration shows a negative influence on the adsorption efficiency.

The ANOVA results conducted on the adsorption model utilizing KOH-activated biochar, which is displayed in Table 4, show that all of the regression terms included in the model were significantly different, signifying a 99% Confidence interval level that the overall regression model is reliable. Further, when the p-value \leq 0.0001, the results show the effect of the independent variables on the response variable (Y) is strong (extremely significant). The response surface plots were developed to evaluate the impact of four main parameters on the dye adsorption process with KOH-activated biochar, where two factors were varied and two factors were kept constant, as shown in Figure 7 (El-Habacha et al., 2024; Aasli et al., 2025; Mahmoudy et al., 2025). Surface and contour mapping

Table 4. ANOVA-based evaluation of model significance

Sorbent	Adsorption capacity	Factors	Variance sum	Df	Mean square	p-value	Significance test
		Regression	2890.1	4	2387.60	≤0.0001	***
BK	Y	Residue	20.3	3	-	-	
		Total	89075.57	26	-	-	

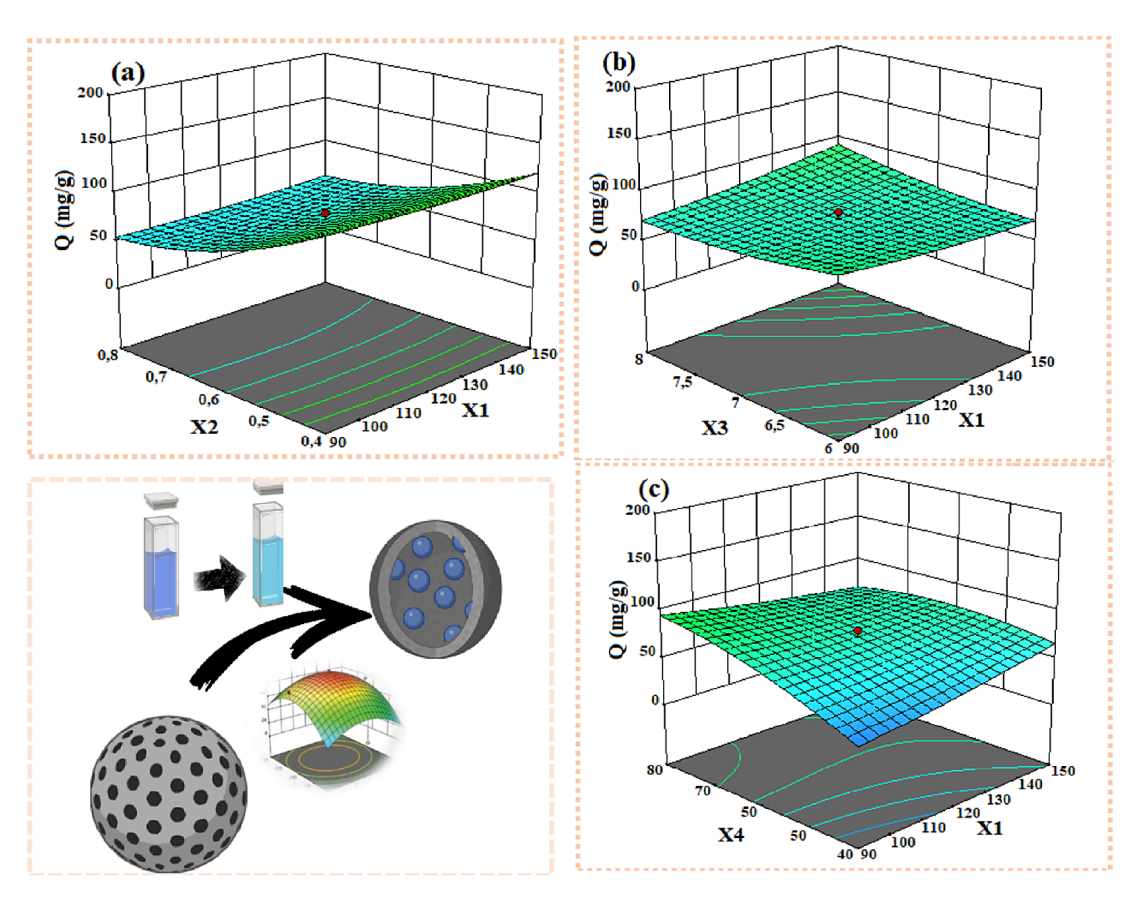


Figure 7. Response surface analysis of MB adsorption using BK

was utilized to illustrate the interaction effects among reaction time, asorbent dose, solution pH, and dye concentration on adsorption capacity. Using Figure 7(a), when considering the amount of adsorbent and contact time, the data indicated that a smaller adsorbent dose actually enhanced adsorption capacity per gram of adsorbent. Though the trend may seem counterintuitive, the increase in per gram adsorption occurs because a lower amount of adsorbent requires a higher loading for a constant dye concentration. Higher amounts of adsorbent provide a greater amount of active bonding sites to remove the pollutant, however there is not a proportional increase in pollutant removal, as there is a constant dye concentration that restricts efficiency of pollutant removal per site used. Contact time increases adsorption as it increases potential for dye intrusion within the adsorbent pore network, allowing adsorbent equilibrium to be attained.

As shown in Figure 7(b), the simultaneous impact of interaction time and solution pH on dye uptake behavior. Increased contact time raises the degree of adsorption associated with the dye molecules being more accessible on the binding sites of the adsorbent. In addition, since the biochar surface is more negatively charged under alkaline conditions, it favors adsorption of the positively charged methylene blue molecules through a stronger electrostatic attraction. In the acidic pH range, the protonation of the surface sites induces repulsive forces that diminish adsorption capacity. The combined effects of contact time and initial dye concentration are shown in Figure 7(c). Longer times allow adsorption to take place as there is increased opportunity for the molecules

to diffuse and to interact with the active sites. Higher initial concentrations also contribute to the increased driving force for mass transfer, which leads to higher dye uptake. More dye molecules available at higher concentrations will also occupy available adsorption sites and overall adsorption capacity will improve.

Figure 8 confirms the predictive ability of the adsorption model developed by comparing predicted adsorption values to experimental values

and showing good agreement. The trendline in Figure 8 demonstrates excellent agreement with predictions and experiments with the points closely clustering about the line of equality. An analysis of the residuals indicates random scatter about zero, confirming that the model predictions are unbiased and reliable (El-Habacha et al., 2024; Aasli et al., 2025; Mahmoudy et al., 2025).

Figure 9 illustrates the connection between adsorption capacity and the cumulative impact

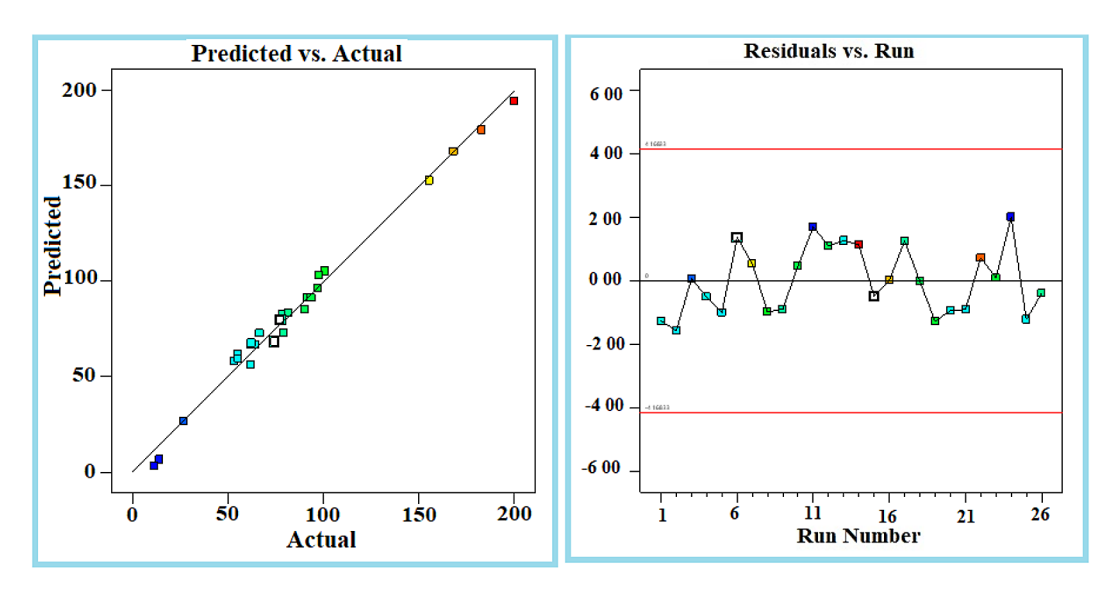


Figure 8. Correlation between predicted and actual adsorption results of BK

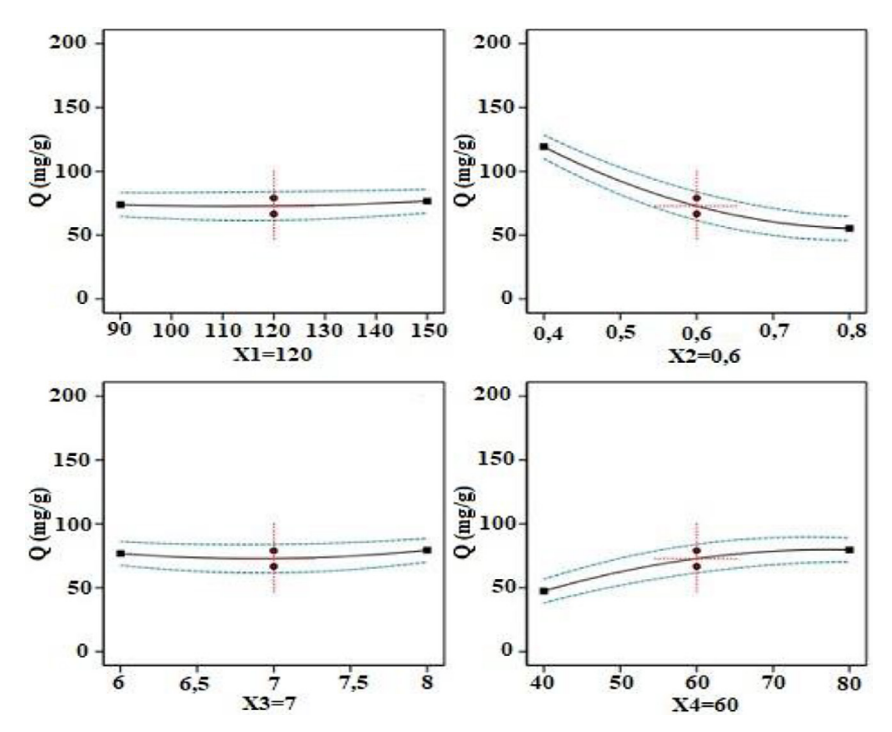


Figure 9. Impact of independent variables on adsorption performance

of time of contact, adsorbent mass, pH, and dye concentration for BK. Regarding contact time, at around 120 minutes, the adsorption capacity appears mostly unchanged with subsequent increases, which means that the system quickly reaches equilibrium. In other words, increasing contact time past this point will not yield significantly increased dye uptake. Conversely, there is an observable negative correlation between quantity of adsorbent and adsorption capacity per unit mass. Adding more activated biochar will lower individual efficiency, potentially due to overlapping of adsorption sites or limited pollutant molecules compared to surface area. The pH of the solution maintained steady performance, close to neutrality. At higher pH, a slight decrease in adsorption efficiency appears, signifying that the activated biochar adsorption abilities are greatest in a near-neutral setting. Increasing the initial dye concentration increases the potential for adsorption capacity, as greater initial dye concentrations likely increase the driving force for the adsorption (Ben Ali et al., 2025).

Results of isotherm modelling

The study of the association between and the MB adsorbate was conducted through the application of several adsorption isotherm models, namely Langmuir, Freundlich, and Sips (Almasi et al., 2017). The results derived Insights into the

sorption mechanisms can be drawn from these models, as well as the surface attributes and adsorption affinities. The results are summarized in Figure 10 and Table 5. The results from the Table 5 suggest that of the error values calculated for each model, the Sips model best describes the removal of methylene blue using activated biochar. Among these, the Sips model yields the lowest sum of squared errors (SSE = 164.04), slightly outperforming the Freundlich model (SSE = 188.11), and substantially better than the Langmuir model (SSE = 849.78). This suggests that the Sips model provides the most accurate statistical representation of the experimental data.

The Sips model, also known as the Langmuir–Freundlich model, is an isotherm equation widely used to describe adsorption on heterogeneous surfaces. It combines the characteristics of the Langmuir model, which assumes adsorption occurs as a monolayer on uniform sites, and the Freundlich model, which better represents adsorption on energetically non-uniform surfaces and accounts for multilayer adsorption. Due to this hybrid nature, the Sips model is particularly well-suited for representing complex adsorption phenomena on porous or functionalized materials, as is the case in this study.

According to the results obtained for the activated biochar (BK), the heterogeneity parameter n_s , equal to 0.31, indicates a high degree of surface heterogeneity. The closer this value is to zero, the

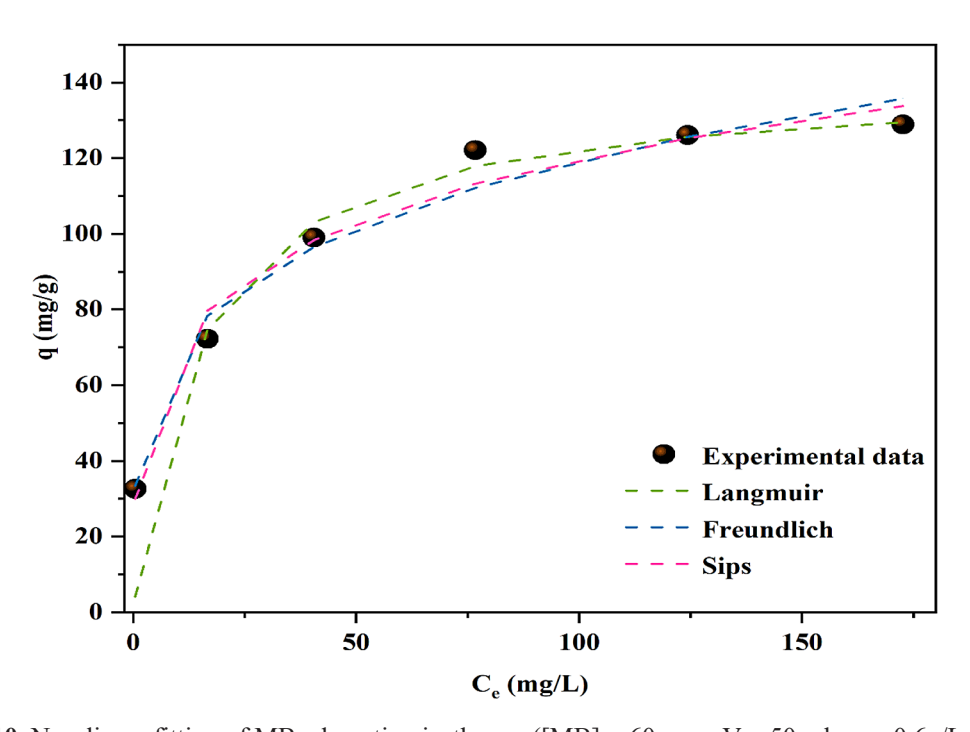


Figure 10. Non-linear fitting of MB adsorption isotherms ([MB] = 60 ppm, V = 50 ml, m = 0.6g/L, pH = 8)

Table 5. Isotherm adsorption conditions

Models	Parameters	BK
	q _m (mg.g ⁻¹)	140.47
Langmuir	K _L (L.mg ⁻¹)	0.068
	SSE	849.78
	n	4.25
Freundlich	K _F (mg/g) (mg/L) ^{-1/n}	40.44
	SSE	188.11
	n _s	0.31
Sips	q _m (mg.g ⁻¹)	349.90
	K _s (L/mg)	0.0012
	SEE	164.04

more energetically diverse the adsorption sites are, which confirms the disordered or irregular nature of the biochar's surface. Furthermore, the estimated maximum adsorption capacity (q_m) is

remarkably high, reaching 349.90 mg/g, which reflects a strong affinity of the activated biochar for methylene blue. The Sips constant K_s, with a value of 0.0012 L/mg, indicates a relatively weak interaction between the adsorbent and the adsorbate at low concentrations. Figure 7 provides a visual comparison between the experimental adsorption data and the isotherm models. It clearly shows that both the Sips model closely follow the experimental trend, whereas the Langmuir model deviates more significantly. This visual confirmation reinforces the conclusion drawn from statistical metrics (Baari et al., 2025; Mechati et al., 2023; Shikuku and Jemutai-Kimosop, 2020b).

Results compiled in Table 6 clearly show that the activated biochar synthesized in the present study possesses a much greater ability to adsorb MB than many other adsorbent materials previously reported in the literature. This

Table 6. Literature-based comparison of methylene blue uptake by different adsorbents

Adsorbents	рН	Mass (g/L)	Q _{max} (mg/g)	Ref
Activated carbon by KOH from urban sludge	8	0.06	81.04	(Ben Ali et al., 2024)
KOH activated biomass waste	8	0.8	136.5	(Jawad et al., 2021)
Activated carbon by Zncl ₂ from rice husk	8	12	9.73	(Sharma et al., 2011)
Activated carbon of spathodea campanulate byH ₃ PO ₄	90	2	86.207	(Dimbo et al., 2024)
Activated agriculture waste by KOH	8	0.03	140.47	In this Study

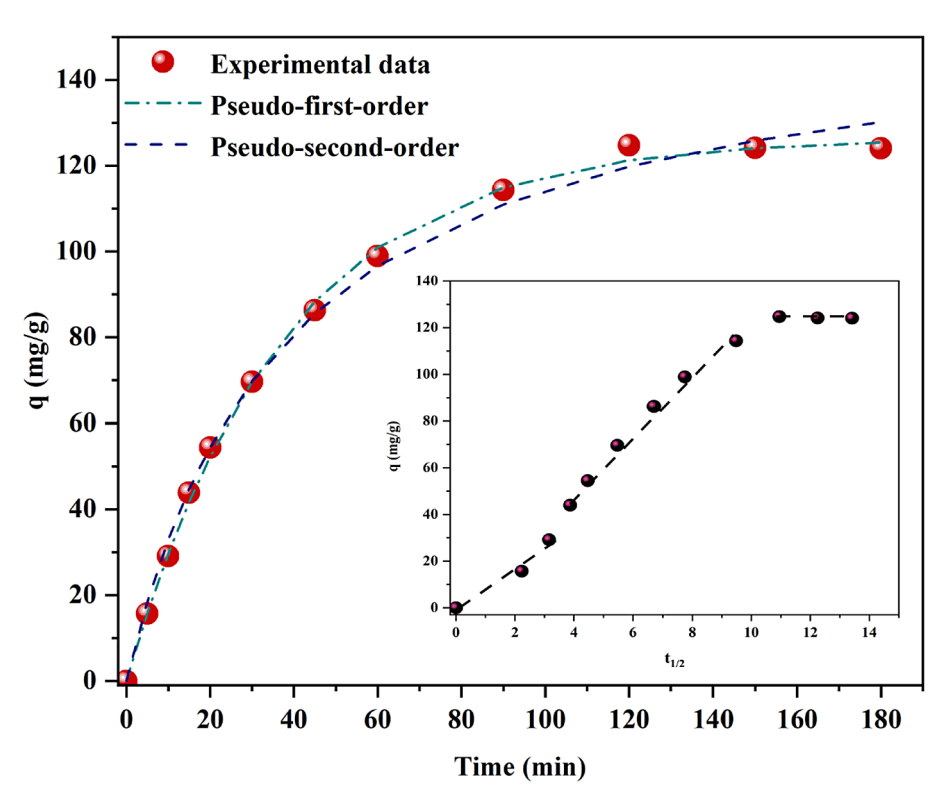


Figure 11. Equilibrium adsorption isotherm of MB ([MB] = 60 ppm, V = 50 ml, mass = 0.6g/L, pH = 8)

Table 7. Kinetic parameters and intra-particle diffusion
for MB adsorption onto BK

Models	Parameters	BK
Pseudo-first-order	K ₁ (min ⁻¹)	0.026
	q _{e,exp}	126.36
	q _{e,th}	112.35
	SSE	32.5
	K ₂ (min ⁻¹)	0.00016
Pseudo-second-order	q _{e,exp}	157.5
Pseudo-second-order	q _{e,th}	125.26
	SSE	105.34
Intro partials diffusion	K _d (mg.g ⁻¹ min ^{-0.5})	6.40
Intra-particle diffusion	С	44.09

comparative evaluation is primarily based on the maximum experimental adsorption capacity, and takes into account similar experimental conditions, particularly in terms of pH and the amount of adsorbent used.

Results of kinetic behaviour and intraparticle mass transfer

Exploration of adsorption kinetics enhances our understanding of the influence of reaction time on adsorption, notably for determining the order of the rate constant. This information is necessary for designing and modelling the adsorption process, and kinetic parameters are considered important. This research focuses on the adsorption of MB on activated carbon at a temperature equal to 298 K (Figure 11).

According to the updated results displayed in Table 7 and visualized in Figure 11, the pseudo-first-order model yielded a rate constant $K_1 = 0.026~\text{min}^{-1}$, with a theoretical adsorption capacity $(q_{\text{e,th}})$ of 112.35 mg/g. This value is fairly similar to the experimental result adsorption capacity $(q_{\text{e,exp}} = 126.36~\text{mg/g})$, suggesting a reasonable fit. Furthermore, the sum of squared errors (SSE = 32.5) supports a moderate concordance between models and experimental data.

In contrast, the pseudo-second-order model, which typically assumes chemisorption playing a dominant role as the rate-limiting stage, yielded a lower rate constant ($K_2 = 0.00016 \; \text{min}^{-1}$) and a higher SSE of 105.34. Despite its higher theoretical adsorption capacity ($q_{\text{e,th}} = 125.26 \; \text{mg/g}$) and experimental value ($q_{\text{e,exp}} = 157.5 \; \text{mg/g}$), the greater deviation indicated by the SSE suggests a weaker fit compared to the pseudo-first-order model in

this specific case (Saha and Grappe, 2017). Table 7 demonstrates that the activated biochar had an intraparticle diffusion constant (K_d) of 6.40 mg·g⁻¹·min^{-0.5} indicating that it took place relatively fast through the pores of the biochar, and additionally, BK had a higher diffusion constant (El-Habacha et al., 2023; Pholosi et al., 2020).

CONCLUSIONS

This study examines the possibility of transforming agricultural waste into activated carbon by thermochemical treatment to create a porous material capable of removing organic pollutants from wastewater, especially dyes from the textile industry. The adsorbents obtained at different stages (agricultural waste, biochar, and BK) Were extensively analyzed using multiple characterization techniques confirmed a significant increase in specific surface area and pore volume, reaching up to 108.022 m²/g after KOH activation. The central composite design methodology was applied for the optimization of adsorption parameters. Kinetic modeling revealed that the experimental data showed a good fit with the pseudo-first-order model. for BK. Regarding adsorption isotherms, the Sips model provided a good fit. Chemical activation with KOH proved to be a key step in enhancing adsorption performance due to its considerable impact on the material's pore structure.

REFERENCES

- Aasli, B., El Messaoudi, N., El Mouden, A., El-Habacha, M., Mahmoudy, G., Miyah, Y., Erraji, F. Z., Knani, S., and Lacherai, A. (2025). Synthesis of urea-formaldehyde resin@chitosan composite for the removal of Congo red from an aqueous solution via adsorption: Box-Behnken design optimization. *International Journal of Biological Macromolecules*, 315, 144648. https://doi.org/10.1016/j.ijbiomac.2025.144648
- Aguiar, J. E., Bezerra, B. T. C., Siqueira, A. C. A., Barrera, D., Sapag, K., Azevedo, D. C. S., Lucena, S. M. P., and Silva, I. J. (2014). Improvement in the adsorption of anionic and cationic dyes from aqueous solutions: a comparative study using aluminium pillared clays and activated carbon. *Separation Science and Technology*, 49(5), 741–751. https://doi.or g/10.1080/01496395.2013.862720
- 3. Al-Asadi, S. T., Mussa, Z. H., Al-Qaim, F. F., Kamyab, H., Al-Saedi, H. F. S., Deyab, I. F., and Kadhim,

- N. J. (2025). A comprehensive review of methylene blue dye adsorption on activated carbon from edible fruit seeds: A case study on kinetics and adsorption models. *Carbon Trends*, 20, 100507. https://doi.org/10.1016/j.cartre.2025.100507
- 4. Alghuthaymi, M. A. (2025). Antifungal action of edible coating comprising artichoke-mediated nanosilver and chitosan nanoparticles for biocontrol of citrus blue Mold. *Polymers*, *17*(12), 1671. https://doi.org/10.3390/polym17121671
- Almasi, A., Rostamkhani, Z., and Mousavi, S. A. (2017). Adsorption of reactive Red 2 using activated carbon prepared from walnut shell: Batch and fixed bed studies. *Desalination and Water Treatment*, 79, 356–367. https://doi.org/10.5004/dwt.2017.20791
- Al-Rumaihi, A., Shahbaz, M., Mckay, G., Mackey, H., and Al-Ansari, T. (2022). A review of pyrolysis technologies and feedstock: A blending approach for plastic and biomass towards optimum biochar yield. *Renewable and Sustainable Energy Reviews*, 167, 112715. https://doi.org/10.1016/j.rser.2022.112715
- Amer, M., Brachi, P., Ruoppolo, G., El-Sharkawy, I., Ahmed, M., Ookawara, S., and Elwardany, A. (2021). Pyrolysis and combustion kinetics of thermally treated globe artichoke leaves. *Energy Conversion and Management*, 246, 114656. https://doi. org/10.1016/j.enconman.2021.114656
- Asfaram, A., Ghaedi, M., Agarwal, S., Tyagi, I., and Kumar Gupta, V. (2015). Removal of basic dye Auramine-O by ZnS:Cu nanoparticles loaded on activated carbon: Optimization of parameters using response surface methodology with central composite design. RSC Advances, 5(24), 18438–18450. https:// doi.org/10.1039/C4RA15637D
- 9. Baari, M. J., Rudi, L., and Harimu, L. (2025). Adsorption isotherms, thermodynamics, and kinetics of activated carbon as adsorbent to water pollutants: A review. *Chimica Techno Acta*, *12*(2), 12214, 8582. https://doi.org/10.15826/chimtech.2025.12.2.14
- Barakat, N. A. M., Mahmoud, M. S., and Moustafa, H. M. (2024). Comparing specific capacitance in rice husk-derived activated carbon through phosphoric acid and potassium hydroxide activation order variations. *Scientific Reports*, 14(1), 1460. https://doi.org/10.1038/s41598-023-49675-0
- 11. Ben Ali, M., Bakhtaoui, Y., Flayou, M., El Hazzat, M., Sifou, A., Dahhou, M., Kacimi, M., Benzaouak, A., and El Hamidi, A. (2025). Adsorption of brilliant cresyl blue using NaOH-activated biochar derived from sewage sludge. *E3S Web of Conferences*, 601, 00087. https://doi.org/10.1051/e3sconf/202560100087
- 12. Ben Ali, M., Benzaouak, A., Tangarfa, M., Abrouki, Y., Belekbir, S., Hazzat, M. El., El Hamidi, A., and Abdelouahed, L. (2025). Multi-response optimization of the adsorption properties of activated carbon

- produced from H2SO4 activated sludge: Effects of washing with HCl. *Case Studies in Chemical and Environmental Engineering*, *11*, 101219. https://doi.org/10.1016/j.cscee.2025.101219
- Ben Ali, M., Benzaouak, A., Valentino, L., Moussadik, A., El Hazzat, M., Abdelouahed, L., El Hamidi, A., and Liotta, L. F. (2025). Copper-decorated Biochar derived from sludge as eco-friendly nano-catalyst for efficient p-nitrophenol reduction. *Catalysis Today*, 459, 115421. https://doi.org/10.1016/j.cattod.2025.115421
- Ben Ali, M., Flayou, M., Boutarba, Y., El Youssfi, M., Bakhtaoui, Y., El Hazzat, M., Sifou, A., Dahhou, M., Kacimi, M., Benzaouak, A., and El Hamidi, A. (2024). Conversion of urban sludge into KOHactivated biochar for methylene blue adsorption. *Moroccan Journal of Chemistry*, 12(4), 1852–1869. https://doi.org/10.48317/IMIST.PRSM/MORJCHEM-V12I4.50578
- 15. Bencheikh, I., Azoulay, K., Mabrouki, J., El Hajjaji, S., Dahchour, A., Moufti, A., and Dhiba, D. (2020). The adsorptive removal of MB using chemically treated artichoke leaves: Parametric, kinetic, isotherm and thermodynamic study. *Scientific African*, 9, e00509. https://doi.org/10.1016/j.sciaf.2020.e00509
- 16. Bencheikh, I., Azoulay, K., Mabrouki, J., El Hajjaji, S., Moufti, A., and Labjar, N. (2021). The use and the performance of chemically treated artichoke leaves for textile industrial effluents treatment. *Chemical Data Collections*, 31, 100597. https://doi.org/10.1016/j.cdc.2020.100597
- 17. Campos, N. F., Barbosa, C. M., Rodríguez-Díaz, J. M., and Duarte, M. M. (2018). Removal of naphthenic acids using activated charcoal: Kinetic and equilibrium studies. *Adsorption Science & Technology*, 36(7–8), 1405–1421. https://doi.org/10.1177/0263617418773844
- 18. Cao, X., Williams, P. N., Zhan, Y., Coughlin, S. A., McGrath, J. W., Chin, J. P., and Xu, Y. (2023). Municipal solid waste compost: Global trends and biogeochemical cycling. *Soil & Environmental Health*, 1(4), 100038. https://doi.org/10.1016/j.seh.2023.100038
- Castagna, A., Aboudia, A., Guendouz, A., Scieuzo, C., Falabella, P., Matthes, J., Schmid, M., Drissner, D., Allais, F., Chadni, M., Cravotto, C., Senge, J., Krupitzer, C., Canesi, I., Spinelli, D., Drira, F., Ben Hlima, H., Abdelkafi, S., Konstantinou, I., ... Coltelli, M.-B. (2025). Transforming agricultural waste from mediterranean fruits into renewable materials and products with a circular and digital approach. *Materials*, 18(7), 1464. https://doi.org/10.3390/ma18071464
- 20. Chen, Y., Peng, N., Gao, Y., Li, Q., Wang, Z., Yao, B., and Li, Y. (2023). Two-stage pretreatment of Jerusalem artichoke stalks with wastewater recycling

- and lignin recovery for the biorefinery of lignocellulosic biomass. *Processes*, *11*(1), 127. https://doi.org/10.3390/pr11010127
- 21. Czerwińska, K., Śliz, M., and Wilk, M. (2022). Hydrothermal carbonization process: Fundamentals, main parameter characteristics and possible applications including an effective method of SARS-CoV-2 mitigation in sewage sludge. A review. *Renewable and Sustainable Energy Reviews*, 154, 111873. https://doi.org/10.1016/j.rser.2021.111873
- 22. Dang, D., Mei, L., Yan, G., and Liu, W. (2023). Synthesis of nanoporous biochar from rice husk for adsorption of methylene blue. *Journal of Chemistry*, 2023, 1–11. https://doi.org/10.1155/2023/6624295
- 23. Dimbo, D., Abewaa, M., Adino, E., Mengistu, A., Takele, T., Oro, A., and Rangaraju, M. (2024). Methylene blue adsorption from aqueous solution using activated carbon of spathodea campanulata. *Results in Engineering*, *21*, 101910. https://doi.org/10.1016/j.rineng.2024.101910
- 24. Dong, X., Chu, Y., Tong, Z., Sun, M., Meng, D., Yi, X., Gao, T., Wang, M., and Duan, J. (2024). Mechanisms of adsorption and functionalization of biochar for pesticides: A review. *Ecotoxicology* and *Environmental Safety*, 272, 116019. https://doi. org/10.1016/j.ecoenv.2024.116019
- 25. El-Habacha, M., Dabagh, A., Lagdali, S., Miyah, Y., Mahmoudy, G., Sinan, F., Chiban, M., Iaich, S., and Zerbet, M. (2023). An efficient and adsorption of methylene blue dye on a natural clay surface: Modeling and equilibrium studies. *Environmental Science and Pollution Research*. https://doi.org/10.1007/s11356-023-27413-3
- 26. El-Habacha, M., Lagdali, S., Dabagh, A., Mahmoudy, G., Assouani, A., Benjelloun, M., Miyah, Y., Iaich, S., Chiban, M., and Zerbet, M. (2024). High efficiency of treated-phengite clay by sodium hydroxide for the Congo red dye adsorption: Optimization, cost estimation, and mechanism study. *Environmental Research*, 259, 119542. https://doi.org/10.1016/j.envres.2024.119542
- 27. ElShafei, G. M. S., ElSherbiny, I. M. A., Darwish, A. S., and Philip, C. A. (2017). Artichoke as a non-conventional precursor for activated carbon: Role of the activation process. *Journal of Taibah University for Science*, *11*(5), 677–688. https://doi.org/10.1016/j. jtusci.2016.04.006
- 28. Escudero-Curiel, S., Giráldez, A., Pazos, M., and Sanromán, Á. (2023). From waste to resource: valorization of lignocellulosic agri-food residues through engineered hydrochar and biochar for environmental and clean energy applications—a comprehensive review. *Foods*, 12(19), 3646. https://doi. org/10.3390/foods12193646
- 29. Eyupoglu, V., Akin, M. B., Kaya, S., Çaylak, O., Berisha, A., and Çetinkaya, S. (2025). Effective

- removal of methylene blue dye from aqueous solution using Macrolepiota procera mushroom: Experimental and theoretical studies. *Journal of Molecular Liquids*, *418*, 126714. https://doi.org/10.1016/j.molliq.2024.126714
- Fakhar, A., Canatoy, R. C., Galgo, S. J. C., Rafique, M., and Sarfraz, R. (2025a). Advancements in modified biochar production techniques and soil application: A critical review. *Fuel*, 400, 135745. https://doi.org/10.1016/j.fuel.2025.135745
- Fakhar, A., Canatoy, R. C., Galgo, S. J. C., Rafique, M., and Sarfraz, R. (2025b). Advancements in modified biochar production techniques and soil application: A critical review. *Fuel*, 400, 135745. https://doi.org/10.1016/j.fuel.2025.135745
- 32. Genuino, D. A. D., De Luna, M. D. G., and Capareda, S. C. (2018). Improving the surface properties of municipal solid waste-derived pyrolysis biochar by chemical and thermal activation: Optimization of process parameters and environmental application. *Waste Management*, 72, 255–264. https://doi.org/10.1016/j.wasman.2017.11.038
- 33. Giertl, T., Vitázek, I., Gaduš, J., Kollárik, R., and Przydatek, G. (2024). Thermochemical Conversion of Biomass into 2nd Generation Biofuel. *Processes*, 12(12), 2658. https://doi.org/10.3390/pr12122658
- 34. Gómez, I. C., Cruz, O. F., Silvestre-Albero, J., Rambo, C. R., and Escandell, M. M. (2022). Role of KCl in activation mechanisms of KOH-chemically activated high surface area carbons. *Journal of CO2 Utilization*, 66, 102258. https://doi.org/10.1016/j.jcou.2022.102258
- 35. Guan, J., Zhu, M., Zhou, J., Luo, L., Fernando Romanholo Ferreira, L., Zhang, X., and Liu, J. (2023). Agricultural waste biochar after potassium hydroxide activation: Its adsorbent evaluation and potential mechanism. *Bioresource Technology*, 389, 129793. https://doi.org/10.1016/j.biortech.2023.129793
- 36. Hajji Nabih, M., El Hajam, M., Boulika, H., Hassan, M. M., Idrissi Kandri, N., Hedfi, A., Zerouale, A., and Boufahja, F. (2021). Physicochemical characterization of cardoon "*Cynara cardunculus*" wastes (Leaves and Stems): A comparative study. *Sustainability*, *13*(24), 13905. https://doi.org/10.3390/su132413905
- 37. Ippolito, J. A., Cui, L., Kammann, C., Wrage-Mönnig, N., Estavillo, J. M., Fuertes-Mendizabal, T., Cayuela, M. L., Sigua, G., Novak, J., Spokas, K., and Borchard, N. (2020). Feedstock choice, pyrolysis temperature and type influence biochar characteristics: A comprehensive meta-data analysis review. *Biochar*, *2*(4), 421–438. https://doi.org/10.1007/s42773-020-00067-x
- 38. Islam, N. F., Gogoi, B., Saikia, R., Yousaf, B., Narayan, M., and Sarma, H. (2024). Encouraging circular economy and sustainable environmental

- practices by addressing waste management and biomass energy production. *Regional Sustainability*, *5*(4), 100174. https://doi.org/10.1016/j.regsus.2024.100174
- Jawad, A. H., Abdulhameed, A. S., Bahrudin, N. N., Hum, N. N. M. F., Surip, S. N., Syed-Hassan, S. S. A., Yousif, E., and Sabar, S. (2021). Microporous activated carbon developed from KOH activated biomass waste: Surface mechanistic study of methylene blue dye adsorption. *Water Science and Tech*nology, 84(8), 1858–1872. https://doi.org/10.2166/ wst.2021.355
- 40. Khan, I., Saeed, K., Zekker, I., Zhang, B., Hendi, A. H., Ahmad, A., Ahmad, S., Zada, N., Ahmad, H., Shah, L. A., Shah, T., and Khan, I. (2022). Review on Methylene Blue: Its Properties, Uses, Toxicity and Photodegradation. *Water*, 14(2), 242. https:// doi.org/10.3390/w14020242
- 41. Kim, S., Lee, S.-E., Baek, S.-H., Choi, U., and Bae, H.-J. (2023). Preparation of activated carbon from Korean anthracite: Simultaneous control of ash reduction and pore development. *Processes*, 11(10), 2877. https://doi.org/10.3390/pr11102877
- 42. Kuryntseva, P., Karamova, K., Galitskaya, P., Selivanovskaya, S., and Evtugyn, G. (2023). Biochar functions in soil depending on feedstock and pyrolyzation properties with particular emphasis on biological properties. *Agriculture*, *13*(10), 2003. https://doi.org/10.3390/agriculture13102003
- 43. Lendzion-Bieluń, Z., Czekajło, Ł., Sibera, D., Moszyński, D., Sreńscek-Nazzal, J., Morawski, A. W., Wrobel, R. J., Michalkiewicz, B., Arabczyk, W., and Narkiewicz, U. (2018). Surface characteristics of KOH-treated commercial carbons applied for CO₂ adsorption. *Adsorption Science & Technology*, 36(1–2), 478–492. https://doi.org/10.1177/0263617417704527
- 44. Li, R., Zhang, W., Yan, S., Zhang, D., and Xu, W. (2025). Degradation of Methylene blue in water using x-PMoV@MnCo2O4-NH2: Synergistic action with peroxymonosulfate and mechanistic insights. *Separation and Purification Technology*, *354*, 129038. https://doi.org/10.1016/j.seppur.2024.129038
- 45. Liu, N., Liu, Z., Wang, Y., Zhou, T., Zhang, M., and Yang, H. (2025). Clean and efficient thermochemical conversion technologies for biomass in green methanol production. *Biomass*, *5*(1), 13. https://doi.org/10.3390/biomass5010013
- 46. Ma, Y., Wang, J., and Zhang, Y. (2018). TG-FTIR study on pyrolysis of *Enteromorpha prolifera*. Biomass *Conversion and Biorefinery*, 8(1), 151–157. https://doi.org/10.1007/s13399-016-0234-6
- 47. Mahmoudy, G., Dabagh, A., El-Habacha, M., Lagdali, S., Assouani, A., Aasli, B., Iaich, S., Chiban, M., and Zerbet, M. (2025). High-efficiency removal of phosphate ions using treated *Carpobrotus edulis*

- biomass: Optimization, mechanism study, cost analysis, and industrial wastewater application. *Scientific African*, 28, e02748. https://doi.org/10.1016/j.sciaf.2025.e02748
- 48. Maitlo, G., Ali, I., Mangi, K. H., Ali, S., Maitlo, H. A., Unar, I. N., and Pirzada, A. M. (2022). Thermochemical conversion of biomass for syngas production: current status and future trends. *Sustainability*, *14*(5), 2596. https://doi.org/10.3390/su14052596
- 49. Mechati, F., Djilani, C., Bougdah, N., Messikh, N., Boussaha, E., Moumen, A., Bouchalta, C., and Medjram, M. S. (2023). Adsorption of methylene blue onto activated carbon prepared under N2/microwave radiation supported cobalt: Kinetics, isotherms, and thermodynamics studies. *Desalination and Water Treatment*, 284, 288–300. https://doi.org/10.5004/dwt.2023.29289
- 50. Morosanu, I., Tofan, L., Teodosiu, C., and Paduraru, C. (2020). Equilibrium studies of the sequential removal of Reactive Blue 19 dye and lead (II) on rapeseed waste. *Revista de Chimie*, 71(7), 162–174. https://doi.org/10.37358/RC.20.7.8234
- 51. Mu, Y., Du, H., He, W., and Ma, H. (2022). Functionalized mesoporous magnetic biochar for methylene blue removal: Performance assessment and mechanism exploration. *Diamond and Related Materials*, 121, 108795. https://doi.org/10.1016/j.diamond.2021.108795
- 52. Mujtaba, M., Fernandes Fraceto, L., Fazeli, M., Mukherjee, S., Savassa, S. M., Araujo De Medeiros, G., Do Espírito Santo Pereira, A., Mancini, S. D., Lipponen, J., and Vilaplana, F. (2023). Lignocellulosic biomass from agricultural waste to the circular economy: A review with focus on biofuels, biocomposites and bioplastics. *Journal of Cleaner Production*, 402, 136815. https://doi.org/10.1016/j.jclepro.2023.136815
- 53. Nematallah, K. A., Albohy, A., and Swilam, N. (2024). Phytotherapeutic approach to enhance the hepatoprotective activity of some edible plants: Molecular docking and nanoformulation. *Journal of Functional Foods*, 122, 106471. https://doi.org/10.1016/j.jff.2024.106471
- 54. Oladoye, P. O., Ajiboye, T. O., Omotola, E. O., and Oyewola, O. J. (2022). Methylene blue dye: Toxicity and potential elimination technology from wastewater. *Results in Engineering*, *16*, 100678. https://doi.org/10.1016/j.rineng.2022.100678
- 55. Perdana, T., Kusnandar, K., Perdana, H. H., and Hermiatin, F. R. (2023). Circular supply chain governance for sustainable fresh agricultural products: Minimizing food loss and utilizing agricultural waste. *Sustainable Production and Consumption*, *41*, 391–403. https://doi.org/10.1016/j.spc.2023.09.001
- 56. Pholosi, A., Naidoo, E. B., and Ofomaja, A. E. (2020). Intraparticle diffusion of Cr(VI) through

- biomass and magnetite coated biomass: A comparative kinetic and diffusion study. *South African Journal of Chemical Engineering*, *32*, 39–55. https://doi.org/10.1016/j.sajce.2020.01.005
- 57. Riseh, R. S., Vazvani, M. G., Hassanisaadi, M., and Thakur, V. K. (2024). Agricultural wastes: A practical and potential source for the isolation and preparation of cellulose and application in agriculture and different industries. *Industrial Crops and Products*, 208, 117904. https://doi.org/10.1016/j.indcrop.2023.117904
- 58. Rivera-Utrilla, J., Bautista-Toledo, I., Ferro-García, M. A., and Moreno-Castilla, C. (2001). Activated carbon surface modifications by adsorption of bacteria and their effect on aqueous lead adsorption: Adsorption of *E coli* on activated carbons. *Journal of Chemical Technology & Biotechnology*, 76(12), 1209–1215. https://doi.org/10.1002/jctb.506
- 59. Saha, D., and Grappe, H. A. (2017). Adsorption properties of activated carbon fibers. In *Activated Carbon Fiber and Textiles* 143–165. Elsevier. https://doi.org/10.1016/B978-0-08-100660-3.00005-5
- 60. Seo, M. W., Lee, S. H., Nam, H., Lee, D., Tokmurzin, D., Wang, S., and Park, Y.-K. (2022). Recent advances of thermochemical conversion processes for biorefinery. *Bioresource Technology*, 343, 126109. https://doi.org/10.1016/j.biortech.2021.126109
- 61. Sharma, Y. C., Uma, and Upadhyay, S. N. (2011). An economically viable removal of methylene blue by adsorption on activated carbon prepared from rice husk. *The Canadian Journal of Chemical Engineering*, 89(2), 377–383. https://doi.org/10.1002/cjce.20393
- 62. Shikuku, V. O., and Jemutai-Kimosop, S. (2020a). Efficient removal of sulfamethoxazole onto sugarcane bagasse-derived biochar: two and three-parameter isotherms, kinetics and thermodynamics. S. Afr. J. Chem.
- 63. Shikuku, V. O., and Jemutai-Kimosop, S. (2020b). Efficient removal of sulfamethoxazole onto sugarcane bagasse-derived biochar: two and three-parameter isotherms, kinetics and thermodynamics. S. Afr. J. Chem.
- 64. Srivatsav, P., Bhargav, B., Shanmugasundaram, V., Arun, J., Gopinath, K., and Bhatnagar, A. (2020). Biochar as an eco-friendly and economical adsorbent for the removal of colorants (Dyes) from aqueous environment: a review. *Water, 12*(12), 3561. https://doi.org/10.3390/w12123561
- 65. Sun, J., Jayakumar, A., Díaz-Maroto, C. G., Moreno, I., Fermoso, J., and Mašek, O. (2024). The role of feedstock and activation process on supercapacitor performance of lignocellulosic biochar. *Biomass and Bioenergy*, *184*, 107180. https://doi.org/10.1016/j.biombioe.2024.107180

- 66. Tangarfa, M., Semlali Aouragh Hassani, N., and Alaoui, A. (2019). Behavior and mechanism of tannic acid adsorption on the calcite surface: isothermal, kinetic, and thermodynamic studies. *ACS Omega*, *4*(22), 19647–19654. https://doi.org/10.1021/acsomega.9b02259
- 67. Tekin, N., Dinçer, A., Demirbaş, Ö., and Alkan, M. (2010). Adsorption of cationic polyacrylamide (C-PAM) on expanded perlite. *Applied Clay Science*, *50*(1), 125–129. https://doi.org/10.1016/j.clay.2010.07.014
- 68. Trivedi, Y., Sharma, M., Mishra, R. K., Sharma, A., Joshi, J., Gupta, A. B., Achintya, B., Shah, K., and Vuppaladadiyamd, A. K. (2025). Biochar potential for pollutant removal during wastewater treatment: A comprehensive review of separation mechanisms, technological integration, and process analysis. *Desalination*, 600, 118509. https://doi.org/10.1016/j.desal.2024.118509
- 69. Unyay, H., Altay, H. O., Perendeci, N. A., Szufa, S., Ozdemir, F., and Angelidaki, İ. (2025). Valorisation potential of black tea processing wastes for bioactive compounds recovery and renewable energy production. *Journal of Environmental Chemical Engineering*, 13(3), 117124. https://doi.org/10.1016/j.jece.2025.117124
- 70. Van Den Broek, S., Nybom, I., Hartmann, M., Doetterl, S., and Garland, G. (2024). Opportunities and challenges of using human excreta-derived fertilizers in agriculture: A review of suitability, environmental impact and societal acceptance. *Science of The Total Environment*, 957, 177306. https://doi.org/10.1016/j.scitotenv.2024.177306
- 71. Wang, X., and Shafieezadeh, M. M. (2025). A decision framework for sustainable industrial water pollution control to protect marine environments. *Marine Pollution Bulletin*, 214, 117726. https://doi.org/10.1016/j.marpolbul.2025.117726
- 72. Wang, Y., and Cui, X. (2024). Modeling and quantification of agricultural waste recycling for agricultural industrial structure optimization in a novelty multi-village industrial complex. *Environmental Impact Assessment Review*, 106, 107484. https://doi.org/10.1016/j.eiar.2024.107484
- 73. Wu, J., Yang, J., Feng, P., Huang, G., Xu, C., and Lin, B. (2020). High-efficiency removal of dyes from wastewater by fully recycling litchi peel biochar. *Chemosphere*, 246, 125734. https://doi.org/10.1016/j.chemosphere.2019.125734
- 74. Yaashikaa, P. R., Kumar, P. S., Varjani, S., and Saravanan, A. (2020). A critical review on the biochar production techniques, characterization, stability and applications for circular bioeconomy. *Biotechnology Reports*, 28, e00570. https://doi. org/10.1016/j.btre.2020.e00570